ANTICORROSIVE PROPERTIES OF $ZnTa_2O_6$ AND ZnV_2O_6 NANOMATERIALS - DEPOSITED AS SANDWICH STRUCTURES BY DROP CASTING METHOD - IN NaCl

BIRDEANU Mihaela[1], BIRDEANU Aurel - Valentin[1, 2], VAIDA Mirela[1], ORHA Corina[1], FAGADAR-COSMA Eugenia[3]

[1]*National Institute for Research and Development in Electrochemistry and Condensed Matter, Timisoara, Romania, EU*
[2]*National R&D Institute for Welding and Material Testing - ISIM Timişoara, Romania, EU*
[3]*Institute of Chemistry Timisoara of the Romanian Academy, Timisoara, Romania, EU*
mihaelabirdeanu@gmail.com

Abstract

$ZnTa_2O6$ and ZnV_2O_6 nanomaterials were obtained by hydrothermal and co-precipitation synthesis methods. Optical measurements (UV-VIS) were realized for $ZnTa_2O_6$ and ZnV_2O_6 nanomaterials. Using the drop casting method sandwich structures of $ZnTa_2O_6$ and ZnV_2O_6 nanomaterials were deposited on steel electrodes. The morphological characteristics for the obtained layers were investigated before the electrochemical measurements by scanning electron microscopy and optical microscopy. Corrosion tests in NaCl 0.1M solution were performed for the deposited layers on steel electrodes and the tests revealed that the best results were obtained for the sandwich structures using hydrothermally obtained $ZnTa_2O_6$ as first layer and $ZnTa_2O_6$ obtained by the co-precipitation method as the second layer, i.e. 88.29% inhibition efficiency.

Keywords: $ZnTa_2O_6$, ZnV_2O_6, electrochemical measurements, inhibition efficiency, anticorrosive properties

1. INTRODUCTION

Steel, which is one of the widely used materials in a lot of industries, is affected by the corrosion process due to interaction with the environment. Replacing steel elements from damaged equipment to prevent accidents and to ensure a good functionality of the assemblies means more expenses [1, 2]. Having as main purpose prevent steel corrosion and to ensure a longer lifetime for steel elements protective techniques such as: electroplating, anodizing, chromating, phosphating or the addition of corrosion inhibitors have been intensively developed [3-5]. It was already reported [6-8] that pseudo-binary oxide materials based on ZnO, such as $ZnTa_2O_6$ and ZnV_2O_6, were obtained using various synthesis methods (sol-gel, solid state, etc.) and that these materials could act as corrosion inhibitors for steel [9-10].

Stimulated by the previously obtained results of our group, some of our results focused on the obtaining of $ZnTa_2O_6$ and ZnV_2O_6 pseudo-binary oxide nanomaterials by using the hydrothermal and co-precipitation methods are presented in this paper. Results referring to anticorrosive properties of the obtained pseudo-binary oxides, deposited on carbon steel disk electrodes using drop casting method and studied in 0.1 M NaCl saline solution are also presented.

2. EXPERIMENTAL

To obtain $ZnTa_2O_6$ and ZnV_2O_6 pseudo-binary oxide nanomaterials two alternative synthesis methods were used: hydrothermal and co-precipitation. The starting precursors used during the synthesis for $ZnTa_2O_6$ were $Zn(CH_3COO)3{\cdot}2H_2O$ and Ta_2O_5 in a stoichiometric ratio 1:1. For the hydrothermal synthesis the precursors were mixed and the pH of the obtained solution was established to 12 with NaOH and put into an oven for 12 h at 250 °C. After the reaction took place, the obtained product was filtered and rinsed with double distilled

water. For the co-precipitation method the only difference is that the settled reaction temperature was 250 °C for 1 h.

To obtain ZnV_2O_6 were used $Zn(CH_3COO)_3 \cdot 2H_2O$ and V_2O_5 in a stoichiometric ratio 1:1. The reaction parameters for both used synthesis methods (hydrothermal and co-precipitation) are the same that were described above and used to obtain $ZnTa_2O_6$. There were listed as $ZnTa_2O_6$ (h) and ZnV_2O_6 (h) the pseudo-binary oxide nanomaterials obtained by hydrothermal method and as $ZnTa_2O_6$ (c) and ZnV_2O_6 (c) the pseudo-binary oxide nanomaterials obtained by the co-precipitation method.

The obtained materials were used for thin films depositions in sandwich structures in different combinations (see **Table 1**) using the drop casting method. The depositions were realized on polished carbon steel electrode disks, 10 mm diameter and 2 mm thick, with the following chemical composition (wt. %): Fe: 98, Al: 0.0309, Cu: 0.311, Si: 0.339, Mn: 0.619, Cr: 0.18, Co: 0.0138, Ni: 0.179, C: 0.165, , Mo: 0.0339, W:<0.05, Pb:<0.05, Nb: 0.0023, Ti:<0.005, V:<0.005, Zr:<0.005, P:<0.005 and S:<0.005.

The diffuse reflectance spectra for each $ZnTa_2O_6$ and ZnV_2O_6 nanomaterials, obtained by both synthesis methods, were recorded at room temperature, in the wavelength range 240÷700 nm using a Lambda 950 UV-Vis-NIR spectrometer. Acquired data were used to estimate the band gap for each sample.

The morphology of the surfaces of the thin films depositions on carbon steel electrode disks was investigated using the scanning electron microscopy (SEM) using a Model Inspect S microscope.

Table 1 Drop casting thin films depositions characteristics

Sample	Target material and deposition order	Deposition Mode
a	$ZnTa_2O_6$ (h) / $ZnTa_2O_6$ (c)	Drop-cast Sandwich type
b	$ZnTa_2O_6$ (h) / ZnV_2O_6 (h)	
c	$ZnTa_2O_6$ (h) / ZnV_2O_6 (c)	
d	$ZnTa_2O_6$ (c) / $ZnTa_2O_6$ (h)	
e	$ZnTa_2O_6$ (c) / ZnV_2O_6 (h)	
f	$ZnTa_2O_6$ (c) / ZnV_2O_6 (c)	
g	ZnV_2O_6 (h) / $ZnTa_2O_6$ (h)	
h	ZnV_2O_6 (h) / $ZnTa_2O_6$ (c)	
i	ZnV_2O_6 (h) / ZnV_2O_6 (c)	
j	ZnV_2O_6 (c) / $ZnTa_2O_6$ (h)	
k	ZnV_2O_6 (c) / $ZnTa_2O_6$ (c)	
l	ZnV_2O_6 (c) / ZnV_2O_6 (h)	

It was also investigated the inhibition efficiency (*IE*) of the thin films depositions by electrochemical measurements. The electrochemical characterization of the modified carbon steel electrode disks was performed using a potentiostat type Voltalab Model PGZ 402. The potentiostat was coupled with a three electrode electrochemical cell comprising: a counter electrode (platinum wire), a reference electrode (a saturated calomel electrode) and working electrodes (bare or drop casting modified carbon steel disks (OL) mounted into a Teflon body to ensure an active surface of 0.28 cm^2). The potentiodynamic measurements were performed by sweeping the potential in the range (-1.3 ÷ -0.6 V range) at a scan rate (*v*) of 1 mV / s and maintaining constant temperature of 23 °C. For the corrosion studies a 0.1 M NaCl saline solution was used and the open circuit potential (OCP) of the modified electrodes was monitored for 30 minutes before polarization.

3. RESULTS AND DISSCUSION

For the nanomaterials obtained using the two synthesis methods, before their depositions on carbon steel disk electrodes, diffuse reflectance spectra were recorded. Converting the acquired data, the absorbance spectra were obtained and the corresponding values were inserted into the Kubelka - Munk equations [11-12]. Thus, was plotted $\{(k/s)\,h\nu\}^2$ vs. $h\nu$ for each sample, as it can be seen in **Figure 1**, and the optical band gaps values were estimated ($h\nu$ represents the photon energy, k represents the absorption coefficient and s is the scattering coefficient).

The estimated values for the optical band gaps of the analyzed nanomaterials are: E_g ($ZnTa_2O_6$ (h)) = 3.22 eV, E_g ($ZnTa_2O_6$ (c)) = 3.24 eV, E_g (ZnV_2O_6 (h)) = 3.19 eV and E_g (ZnV_2O_6 (c)) = 3.12 eV.

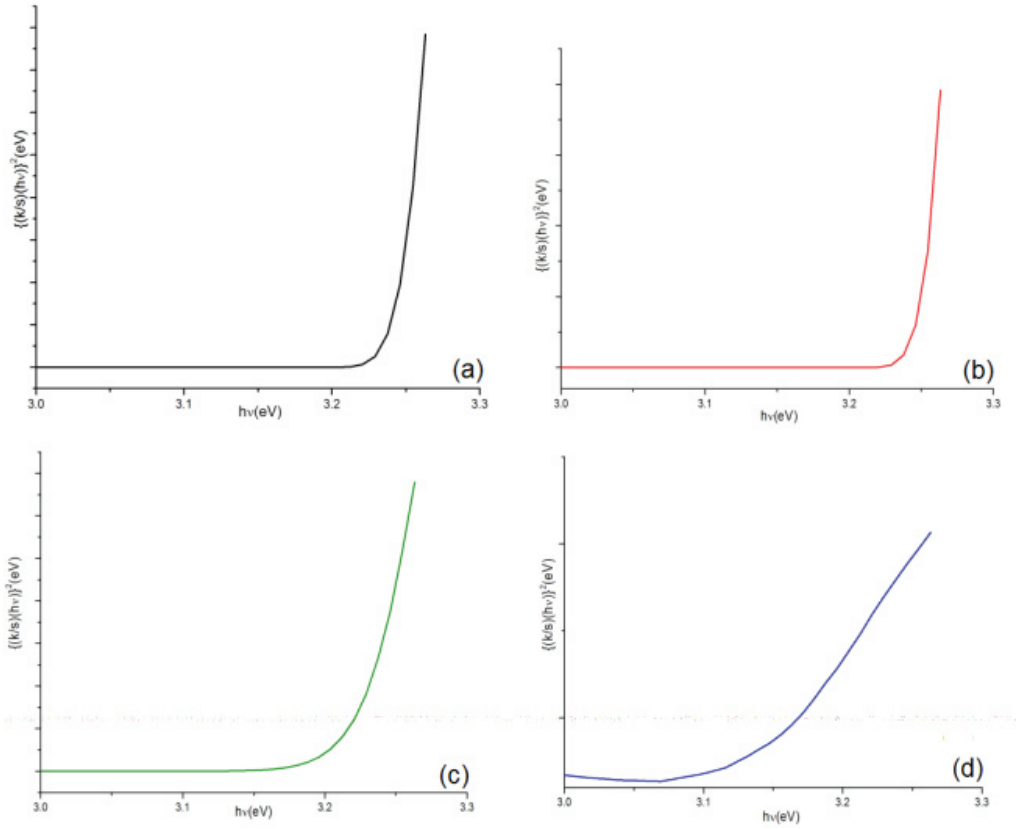

Figure 1 The obtained optical band gaps for each material before the drop casting depositions: a) $ZnTa_2O_6$ (h); b) $ZnTa_2O_6$ (c), c) ZnV_2O_6 (h); d) ZnV_2O_6 (c)

Figure 2 presents the SEM micrographs of the obtained thin films on carbon steel disk electrodes, by deposition of the obtained nanomaterials in sandwich-type structures, using the drop casting method.

As it can be seen from **Figure 2**, the deposited particles that are present on the surface of the carbon steel electrodes form irregular agglomerations. For the realized depositions which involve ZnV_2O_6 hydrothermally obtained, it can be observed that spherical particles are combined with rode shapes particles. Morphologies that are mimicking natural plants were generated, looking like: blowball (dandelion) as shown in **Figure 2-h** and **i** or like cabbage as presented in **Figure 2k**.

In **Figure 3** is presented the evolution of the open circuit potential versus time for bare OL and modified carbon steel disk electrodes in 0.1 M NaCl saline solution for 30 minutes. It is observed that the OCP for the modified electrodes shifts to more positive values comparing with bare OL's OCP. Also, is observed that around 1000 s, some of the deposited sandwich structures are stabilized **Figures 3 (a, b, i, f, g)** while some are constantly decreasing in potential **Figures 3 (c, h, l).**

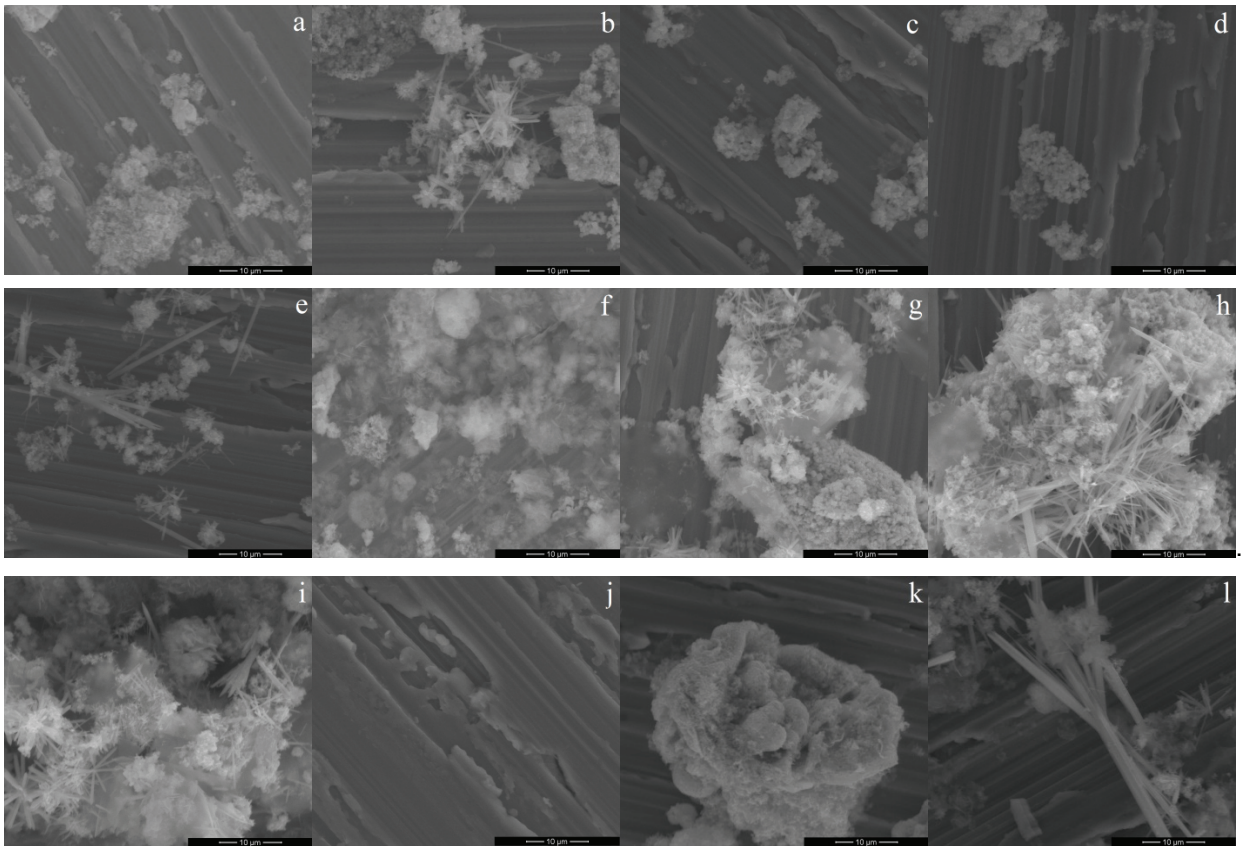

Figure 2 SEM micrographs for the deposited materials in sandwich layers: a) $ZnTa_2O_6$ (h) / $ZnTa_2O_6$ (c); b) $ZnTa_2O_6$ (h) / ZnV_2O_6 (h); c) $ZnTa_2O_6$ (h) / ZnV_2O_6 (c); d) $ZnTa_2O_6$ (c) / $ZnTa_2O_6$ (h); e) $ZnTa_2O_6$ (c) / ZnV_2O_6 (h); f) $ZnTa_2O_6$ (c) / ZnV_2O_6 (c); g) ZnV_2O_6 (h) / $ZnTa_2O_6$ (h); h) ZnV_2O_6 (h) / $ZnTa_2O_6$ (c); i) ZnV_2O_6 (h) / ZnV2O6 (c); j) ZnV_2O_6 (c) / $ZnTa_2O_6$ (h); k) ZnV_2O_6 (c) / $ZnTa_2O_6$ (c) and l) ZnV_2O_6 (c) / ZnV_2O_6 (h)

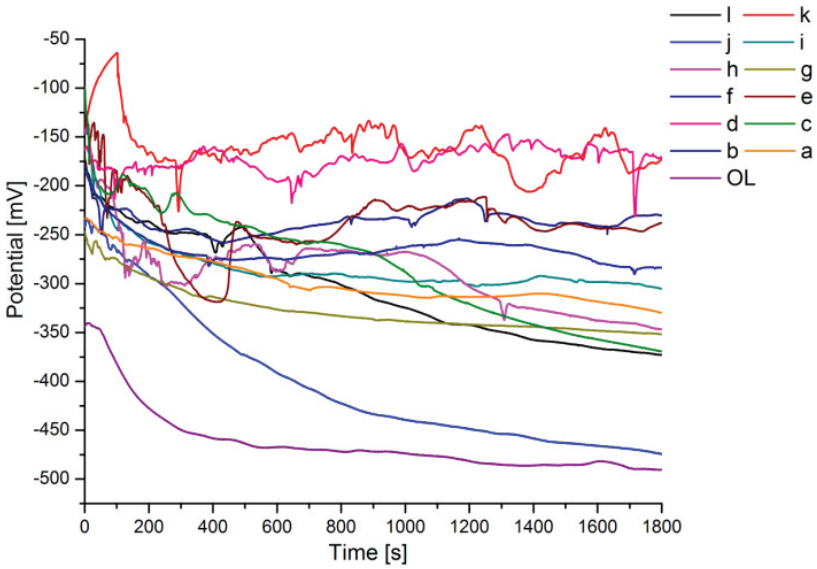

Figure 3 Evolution of open circuit potential with time for the investigated electrodes in 0.1 M NaCl saline solution for: OL (bare electrode), a) $ZnTa_2O_6$ (h) / $ZnTa_2O_6$ (c); b) $ZnTa_2O_6$ (h) / ZnV_2O_6 (h); c) $ZnTa_2O_6$ (h) / ZnV_2O_6 (c); d) $ZnTa_2O_6$ (c) / $ZnTa_2O_6$ (h); e) $ZnTa_2O_6$ (c) / ZnV_2O_6 (h); f) $ZnTa_2O_6$ (c) / ZnV_2O_6 (c); g) ZnV_2O_6 (h) / $ZnTa_2O_6$ (h); h) ZnV_2O_6 (h) / $ZnTa_2O_6$ (c); i) ZnV_2O_6 (h) / ZnV_2O_6 (c); j) ZnV_2O_6 (c) / $ZnTa_2O_6$ (h); k) ZnV_2O_6 (c) / $ZnTa_2O_6$ (c) and l) ZnV_2O_6 (c) / ZnV_2O_6 (h)

Tafel representation of polarization curves for the studied electrodes are represented in **Figure 4** and the summarized Tafel parameters according to the electrochemical measurements are presented in **Table 2**.

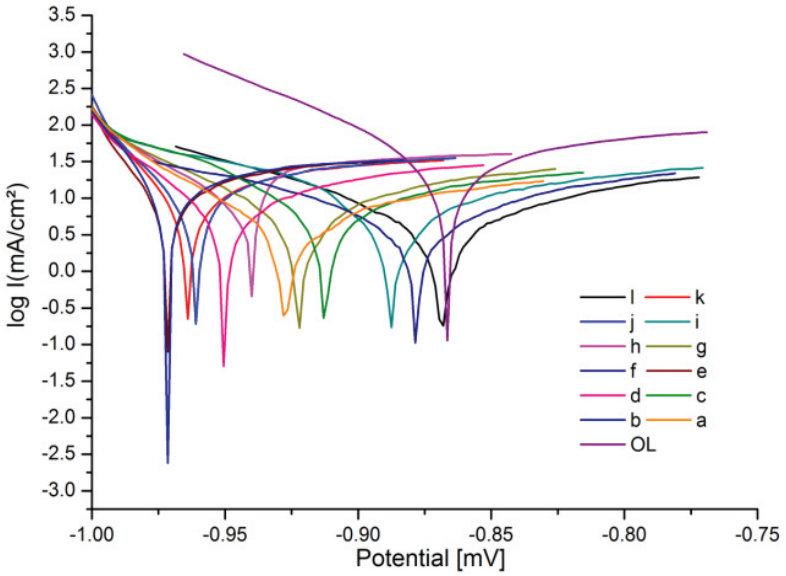

Figure 4 Tafel representation of polarization curves recorded in 0.1 M NaCl saline solution for the investigated electrodes: OL (bare electrode); a) $ZnTa_2O_6$ (h)/ $ZnTa_2O_6$ (c); b) $ZnTa_2O_6$ (h) / ZnV_2O_6 (h); c) $ZnTa_2O_6$ (h) / ZnV_2O_6 (c); d) $ZnTa_2O_6$ (c) / $ZnTa_2O_6$ (h); e) $ZnTa_2O_6$ (c) / ZnV_2O_6 (h); f) $ZnTa_2O_6$ (c) / ZnV_2O_6 (c); g) ZnV_2O_6 (h) / $ZnTa_2O_6$ (h); h) ZnV_2O_6 (h) / $ZnTa_2O_6$ (c); i) ZnV_2O_6 (h) / ZnV2O6 (c); j) ZnV_2O_6 (c) / $ZnTa_2O_6$ (h); k) ZnV_2O_6 (c) / $ZnTa_2O_6$ (c) and l) ZnV_2O_6 (c) / ZnV_2O_6 (h).

The Tafel parameters were calculated using VoltaMaster 4 v.7.09 software and the inhibition efficiency (*IE*) was calculated based on the equation reported in [13]. It was found that the corrosion potential E_{corr} decrease from -866.4 mV (the corresponding current density i_{corr} = 28.7318 µA / cm^2) for the bare OL to -971.7 (i_{corr} = 12.5647 µA / cm^2) for the depositions with $ZnTa_2O_6$ (c) as first layer and ZnV_2O_6 (h) as second layer.

Table 2 The Tafel parameters for bare OL and modified electrodes after 30 minutes immersion in 0.1 M NaCl saline solution

Electrode	E (i=0) (mV)	R_p (kΩ·cm^2)	I_{corr} (µA/cm^2)	β_a (mV)	β_c (mV)	V_{corr} (µm/y)	IE (%)
OL	-866.4	0.5839	28.7318	184.3	-65.7	336.0	-
$ZnTa_2O_6$ (h) / $ZnTa_2O_6$ (c)	**-926.0**	**4.58**	**3.3639**	**290.3**	**-52.8**	**39.34**	**88.29**
$ZnTa_2O_6$ (h) / ZnV_2O_6 (h)	-971.0	0.912	22.1579	481.1	-19.7	259.1	22.88
$ZnTa_2O_6$ (h) / ZnV_2O_6 (c)	-912.2	2.38	10.7117	294.8	-95.3	125.2	62.71
$ZnTa_2O_6$ (c) / $ZnTa_2O_6$ (h)	-949.8	1.87	4.2930	73.2	-36.7	58.21	85.05
$ZnTa_2O_6$ (c) / ZnV_2O_6 (h)	-971.7	1.06	12.5647	150.4	-19.7	146.9	56.26
$ZnTa_2O_6$ (c) / ZnV_2O_6 (c)	-878.3	3.90	4.3328	110.0	-103.6	50.67	84.91
ZnV_2O_6 (h) / $ZnTa_2O_6$ (h)	-921.6	2.52	4.4336	90.8	-58.7	51.85	84.56
ZnV_2O_6 (h) / $ZnTa_2O_6$ (c)	-943.2	1.10	7.1008	117.1	-48.3	83.05	75.28
ZnV_2O_6 (h) / ZnV2O6 (c)	-888.0	2.77	11.0678	297.0	-138.9	129.4	61.47
ZnV_2O_6 (c) / $ZnTa_2O_6$ (h);	-962.0	1.09	17.1487	280.8	-24.1	200.5	40.31
ZnV_2O_6 (c) / $ZnTa_2O_6$ (c)	-963.7	1.15	3.9217	46.2	-22.2	45.86	86.35
ZnV_2O_6 (c) / ZnV_2O_6 (h)	-868.3	3.73	4.8585	145.0	-98.5	56.82	83.09

The deposited layers of $ZnTa_2O_6$ (h) / $ZnTa_2O_6$ (c) on modified carbon steel disk electrode present the best inhibition efficiency, i. e. 88.29 %. The highest polarization resistance (R_p) increase from 0.5839 kΩ·cm^2 for bare OL to 4.58 kΩ·cm^2 which corresponds to the sandwich structure with the highest *IE*. Also, in **Table 2** are presented the values for the Tafel slopes, β_a - the anodic Tafel slope which was found to be larger than the cathodic Tafel slope - β_c for each realized deposition.

4. CONCLUSION

ZnV_2O_6 and $ZnTa_2O_6$ pseudo-binary oxide nanomaterials were obtained using the hydrothermal and the co-precipitation methods. In the case of the deposited layers involving HV nanomaterials, alongside the spherical particles agglomerations was observed rods like shape particles and blowball structures. The optical band gaps estimation showed values of 3.1 ÷ 3.2 eV for the obtained nanomaterials.

The performed corrosion tests in 0.1 M NaCl saline solution revealed that the best result in corrosion inhibition i.e. 88.29 % inhibition efficiency was obtained for the sandwich structures using as first layer $ZnTa_2O_6$ hydrothermally obtained and as second layer $ZnTa_2O_6$ obtained by co-precipitation method.

ACKNOWLEDGEMENTS

The authors kindly acknowledge Romanian financing agency UEFISCDI- PN III No. 107 PED / 2017 project - CorOxiPor: Nanostructured anticorrosive hybrid materials based on pseudo-binary oxides and Zn-metalloporphyrins and Programme 3 from ICT-Romanian Academy.

REFERENCES

[1] GUPTA, R. K., BIRBILIS, N., The influence of nanocrystalline structure and processing route on corrosion of stainless steel: A review, *Corrosion Science,* 2015, vol. 92, pp. 1-15.

[2] AIT HADDOU, B., CHEBABE, D., EL ASSYRY, A., DERMAJ, A., TOUIL, M., IBN AHMED, S., HAJJAJI, N., Experimental and theoretical investigation of 3-methyl-1,2,4-triazole-5-thione derivatives as inhibitors for mild steel corrosion in acid medium, *Journal of Materials and Environmental Sciences*, 2017, vol. 8, no. 11, pp. 3943-3952.

[3] SHABAN, A., FELHOSI, I., TELEGDI, J., Laboratory assessment of inhibition efficiency and mechanism of inhibitor blend (P22SU) on mild steel corrosion in high chloride containing water, *International Journal of Corrosion Scale Inhibition*, 2017, vol. 6, no. 3, pp. 262-275.

[4] PALOU, R.M., OLIVARES-XOLELT, O., LIKHANOVA, N. V., Environmentally Friendly Corrosion Inhibitors, in: Developments in Corrosion Protection, Ed. Dr. M. Aliofkhazraei, Ch. 19, InTech, 2014, pp. 431-465.

[5] LI, Y., CHENG, F., In-situ characterization of the early stage of pipeline steel corrosion in bicarbonate solutions by electrochemical atomic force microscopy, *Surface and Interface Analysis*, doi: 10. 1002/sia.6071

[6] LIU, H., TANG, D., Synthesis of ZnV_2O_6 powder and its cathodic performance for lithium secondary battery, *Materials Chemistry and Physics*, 2009, vol. 114, pp. 656-659.

[7] TANG, R., LI, Y., LI, N., HAN, D., LI, H., ZHAO, Y., GAO, C., ZHU, P., WANG, X., Reversible Structural Phase Transition in ZnV_2O_6 at High Pressures, *The Journal of Physical Chemistry C*, 2014, vol. 118, no. 20, pp. 10560-10566.

[8] JOSHI, R., KUMAR, P., GAUR, A., ASOKAN, K., Structural, optical and ferroelectric properties of V doped ZnO, *Applied Nanoscience*, 2014, vol. 4, no. 5, pp. 531-536.

[9] BIRDEANU, M., FAGADAR-COSMA, G., SEBARCHIEVICI, I., BÎRDEANU, A. - V., TARANU, B., TARANU, I., FAGADAR-COSMA, E., $Zn(Ta_{1-x}Nb_x)_2O_6$ nanomaterials. Synthesis, characterization and corrosion behaviour, *Journal of the Serbian Chemical Society*, 2015, vol. 80, no. 2, pp.895-898.

[10] BIRDEANU, M., BÎRDEANU, A. - V., POPA, I., TARANU, B., PETER, F., CREANGA, I., PALADE, A., FAGADAR-COSMA, E., Comparative Research Regarding Corrosion Protective Effect of Different sandwich type nanostrutures obtained from porphyrins and pseudo-binary oxides by hanging the Deposition Order, in NANOCON 2014: 6th International Conference on Nanomaterials,Brno, Czech Republic, 2014, pp.

[11] KUBELKA, P., MUNK, F., Ein Beitrag Zur Optik Der Farbanstriche, *Zeitschrift für Technische Physik*, 1931, vol. 12, pp. 593-601.

[12] KUBELKA, P., New Contributions to the Optics of Intensely Light-Scattering Materials. Part I, *Journal of Optical Society America*, 1948, vol. 38, pp. 448-457.

[13] AHMAD, Z. Principles of Corrosion Engineering and Corrosion Control, Butterworth-Heinemann/IChemE Series. Elsevier, Amsterdam. 2006. page 377.